

# Appendix from M. S. Shocket et al., “Temperature Drives Epidemics in a Zooplankton-Fungus Disease System: A Trait-Driven Approach Points to Transmission via Host Foraging” (Am. Nat., vol. 191, no. 4, p. 435)

## Additional Methods and Results

In this appendix, we detail our methods and results. (1) We describe the calculations of lake water temperature from the field survey. (2) We show thermal reaction norms for growth rate for several host clones, including the one used in this study. (3) We explain the trait assay experimental methods and trait calculations in greater detail. (4) We show results for the intrinsic growth rate ( $r$ ) and birthrate ( $b$ ) of uninfected hosts as functions of temperature. Those traits are needed to calculate conversion efficiency ( $e$ ) of hosts. (5) We provide the methods used for the sensitivity analysis of the  $R_0$  model of disease spread and include a thorough analysis of the multiple pathways whereby host foraging rate can affect disease spread. (6) We address an apparent discrepancy between the density of algal resources predicted by the dynamical model and observed in the mesocosms. (7) Finally, we describe the methods for analyzing spore load from natural epidemics. The data and code for all analyses in this article are deposited in the Dryad Digital Repository: <http://doi.org/10.5061/dryad.3k8m3> (Shocket et al. 2018).

## Field Survey

### 1. Calculations of Lake Water Temperature

We calculated two measures of water temperature that correspond to differing assumptions about vertical migration of hosts. These measures then incorporate temperature according to predicted habitat use. *Daphnia dentifera* often exhibit diel vertical migration: they spend daytime hours in the lower, colder layer of water (hypolimnion) and migrate to the warmer, top layer of water (epilimnion) at night (Hall et al. 2005). However, preliminary data indicate that for some lakes in our field survey in autumn, some or even most hosts only inhabit the epilimnion (S. R. Hall, unpublished data). Thus, we calculated (1) mean epilimnetic temperature (i.e., no vertical migration, a warmer measure) and (2) a time-weighted temperature based on the typical diel vertical migration pattern (a cooler measure). In reality, most lakes likely fall somewhere between these two extremes.

For each sampling visit, we measured water temperature and dissolved oxygen at 0.5- to 1-m intervals with a Hydrolab multiprobe (Hach Environmental, Loveland, CO). We interpolated temperature and dissolved oxygen data at 0.1-m intervals using a piecewise cubic hermite interpolating polynomial (pchip; Matlab, ver. 7.8 R2009a, MathWorks). We defined the bottom of the epilimnion as the depth at which temperature decreased by  $>1^\circ\text{C m}^{-1}$ . We defined the bottom of the habitable portion of the hypolimnion as the depth at which dissolved oxygen levels dropped  $<1$  ppm (Tessier and Welser 1991). We calculated the temperature for both layers (epilimnion and habitable portion of the hypolimnion) by averaging the temperature spline for all depths within the layer. For the weighted temperature calculation, we weighted the contribution of both layers by time spent in the upper layer (night) vs. lower one (day), a changing proportion from summer to early winter.

## Trait Measurements

### 2. Thermal Reaction Norms among Clones

There is often genetic variation for thermal reaction norms (e.g., Mitchell et al. 2005). We were unable to include multiple genotypes in the trait assays used to parameterize the  $R_0$  model due to logistical constraints on the size of the experiment. However, here we include data showing the thermal reaction norms for one trait (juvenile growth rate) across five *Daphnia dentifera* genotypes, including the clone used in the trait assays and mesocosm experiment (standard). Juvenile growth rate measures the daily rate of change of mass for juvenile *Daphnia* and is generally considered to be proportional to the intrinsic population growth rate ( $r$ ) of a genotype (Lampert and Trubetskova 1996). The standard

clone (light brown) used here is a fast grower overall but shows a fairly typical thermal reaction norm (fig. A1). Hence, it provided us with a highly susceptible and fast-growing clone (Hall et al. 2010a, 2012) with representative thermal response (index by growth rate).

### 3. Experimental Methods and Trait Calculations

#### FORAGING RATE ASSAY

We measured the size- and temperature-dependent foraging rate of hosts by comparing the fluorescence of ungrazed and grazed algae across gradients of host body size and temperature (Sarnelle and Wilson 2008; Penczykowski et al. 2014b). Hosts were cultured in constant temperature environments at 16.2°, 18.4°, 20.9°, 23.7°, and 26.8°C for at least two generations under standard conditions (filtered lake water changed weekly, fed 1.0 mg dry mass/L of a different but still nutritious alga [*Ankistrodesmus* sp.] daily). For the assay, 22 individuals were selected from each temperature that spanned a size gradient including adults, large juveniles, and small juveniles. The animals were transferred individually into centrifuge tubes containing 15 mL of filtered lake water and 1.0 mg dry mass/L algae. We also included 11 control tubes for each temperature that contained algae only. The tubes were returned to the constant temperature environments, kept dark, and inverted every 30 min to resuspend algae. After grazing for 8.5 h, hosts were removed and measured (for body length  $L$ : eye to base of tail spine at  $\times 50$ ); we measured in vivo fluorescence of the remaining algae (Trilogy Laboratory Fluorometer, Turner Designs, San Jose, CA).

#### ESTIMATING FORAGING RATE ( $f$ )

We estimated foraging rate ( $f$ ) as part of the process of fitting size-dependent and temperature-dependent functions in JAGS. We based our estimation on a simplified version of equation (1d). We assumed there was no algal growth during the dark assay. Thus, with only a single susceptible host ( $S$ ) per tube, the differential equation for algae (modified from eq. [1e]) becomes

$$\frac{dA}{dt} = -fSA. \quad (\text{A1})$$

Solving this exponential equation for resource density ( $A$ ) yields

$$A_{\text{rem}} = A_{\text{init}}e^{-fSt_e}, \quad (\text{A2a})$$

where  $A_{\text{rem}}$  is the remaining algae,  $A_{\text{init}}$  is the initial amount of algae (at time  $t = 0$ ),  $S$  is the density of hosts (i.e.,  $1/V$ , where  $V$  is the experiment volume), and  $t_e$  is the duration of the trial ( $\sim 8.5$  h). We fit our model using the log-transformed version of equation (A2a):

$$\ln(A_{\text{rem}}) = \ln(A_{\text{init}}) - fSt_e, \quad (\text{A2b})$$

where residuals,  $\ln(A_{\text{rem}}) - \ln(A_{\text{obs}})$ , were normally distributed on a log scale and  $A_{\text{obs}}$  is the observed remaining algae from grazed tubes.

#### INFECTION ASSAY

We used an infection assay to measure transmission rate ( $\beta$ ). Female adult hosts reared at 20°C were placed in filtered lake water, and offspring were harvested after 24 h. Offspring were collected and reared collectively for 4 days at 20°C. On day 5, we measured the body size of a subset of hosts with a dissecting microscope ( $\times 50$ , average body length = 1.5 mm). We divided hosts into five temperature treatments: 15°, 18°, 20°, 22°, and 25°C. For each temperature treatment, 12 replicate beakers (six hosts per beaker) were filled with 100 mL of filtered lake water for a 24-h exposure to a moderate spore dose (100 spores/mL). The spores used in each temperature treatment were produced by hosts growing at the matching temperature (i.e., 15°C hosts received spores made at 15°C, 18°C hosts received spores made at 18°C, etc., but the 25°C treatment received 22°C spores). All hosts were fed 2.0 mg dry mass/L algae (*Scenedesmus acutus*) daily until visual diagnosis ( $\times 20$ – $\times 50$ ) 10–14 days postexposure.

### ESTIMATING TRANSMISSION RATE ( $\beta$ )

We estimated transmission rate for large adults ( $\beta_{\text{adult}}$ ) as part of the process of fitting temperature-dependent functions in JAGS. We based our estimation on a simplified version of equation (1a) (Bertram et al. 2013), where susceptible hosts ( $S$ ) are lost (and become infected) after contacting spores ( $Z$ ) with transmission rate  $\beta$ :

$$\frac{dS}{dt} = -\beta ZS. \quad (\text{A3})$$

We solve this equation for the remaining susceptible hosts ( $S_{\text{rem}}$ ) after exposure time  $t_e$ , yielding

$$S_{\text{rem}} = S_{\text{init}} e^{-\beta Z t_e}, \quad (\text{A4})$$

where  $S_{\text{init}}$  is the initial numbers of hosts in a beaker. We then use a binomial distribution in our likelihood function to model the number of uninfected hosts in each beaker, where the probability of remaining uninfected ( $P_{\text{uninf}}$ ) is equal to

$$p_{\text{uninf}} = e^{-\beta Z t_e} \quad (\text{A5})$$

and  $\beta$  is a function of temperature ( $T$ ) according to equation (2).

### LIFE TABLE EXPERIMENT

We used a life table experiment to measure the death rates of uninfected and infected hosts ( $d$  and  $d_i$ , respectively), host intrinsic rate of increase ( $r$ ), and maximal spore yield ( $\sigma_{\text{max}}$ ). Individuals for the experiment were collected within a 24-h window from females reared at 20°C in filtered lake water. Hosts were reared collectively for 4 days at 20°C and then placed individually into beakers with 100 mL of filtered lake water. They were then divided into five temperature treatments: 15°, 18°, 20°, 22°, and 26°C. At each temperature, 15 hosts were exposed to parasites (1,000 spores/mL for 24 h), while 10 remained unexposed. Afterward, all hosts were transferred to fresh medium daily (filtered lake water, 2.0 mg dry mass/L *S. acutus*). Offspring were counted daily. We diagnosed infection status of dead hosts; infected hosts were homogenized to estimate spore yield (counted at  $\times 200$  with a hemocytometer). The experiment ended after all of the infected hosts had died (36 days).

### ESTIMATING HOST UNINFECTED AND INFECTED DEATH RATES ( $d$ AND $d_i$ )

We estimated death rate for uninfected ( $d$ ) and infected ( $d_i$ ) hosts as part of the process of fitting temperature-dependent functions in JAGS. We assumed that time until death followed an exponential distribution; thus, the likelihood ( $\ell$ ) of a constant death rate ( $d$ ) is calculated from the time-until-death data ( $t_d$ ) according to

$$\ell(d|t_d) = d e^{-d t_d}. \quad (\text{A6})$$

Not all uninfected hosts died during the life table experiment. Thus, our time-until-death data for the uninfected death rate ( $d$ ) was right-censored. We implemented analysis of censored data using the dinterval distribution in JAGS (JAGS, ver. 3.4.0, user manual: Plummer 2013).

### ESTIMATING HOST INTRINSIC GROWTH RATE ( $r$ ) AND BIRTHRATE ( $b$ )

We estimated the intrinsic rate of increase ( $r$ ) for each unexposed host individual. We solved the standard Euler-Lotka equation according to

$$1 = \sum_t e^{-r t} l_t F_t. \quad (\text{A7})$$

Typically,  $l_t$  is the proportion of animals in a cohort surviving to day  $t$  and  $F_t$  is the average fecundity of the cohort on day  $t$ . In our simplified version for a single individual,  $l_t$  is always equal to 1 (while still alive) and  $F_t$  is the number of offspring produced on day  $t$ , producing the equation

$$1 = \sum_t e^{-r t} F_t, \quad (\text{A8})$$

which is calculated for each individual host. With these calculations, we then estimated temperature-dependent functions for  $r$ .

Birthrate ( $b$ ) is calculated as the sum of intrinsic rate of increase ( $r$ ) and background death rate ( $d$ ) of uninfected hosts:  $b = r + d$ . There was no cost of infection on host birthrate.

#### 4. Results for Host Intrinsic Rate of Increase ( $r$ ) and Birthrate ( $b$ )

Host intrinsic rate of increase ( $r$ ) and birthrate ( $b$ ) both increase over the entire temperature range, both by factors of 1.7 (fig. A2).

### Predicting Disease Spread ( $R_0$ )

#### 5. Sensitivity Analysis

We calculated the contribution of each trait as it appears in equation (5) to the change in  $R_0$  by calculating the partial derivative of  $R_0$  with respect to each trait, scaled per unit of  $R_0$ , and multiplied by the derivative of the trait with respect to temperature (eq. [7]). The derivatives for  $R_0$  with respect to each trait scaled per unit of  $R_0$  are

$$\frac{1}{R_0} \frac{\partial R_0}{\partial \beta} = \frac{1}{\beta}, \quad (\text{A9a})$$

$$\frac{1}{R_0} \frac{\partial R_0}{\partial \sigma_{\max}} = \frac{1}{\sigma_{\max}}, \quad (\text{A9b})$$

$$\frac{1}{R_0} \frac{\partial R_0}{\partial f} = \frac{S_b^*}{S_b^* f + m}, \quad (\text{A9c})$$

$$\frac{1}{R_0} \frac{\partial R_0}{\partial A_b^*} = \frac{h}{A_b^*(A_b^* + h)}, \quad (\text{A9d})$$

$$\frac{1}{R_0} \frac{\partial R_0}{\partial S_b^*} = \frac{m}{S_b^*(S_b^* f + m)}. \quad (\text{A9e})$$

The derivatives for each trait with respect to temperature are calculated either directly from the temperature-dependent functions (for  $\sigma_{\max}$  and  $f$ ; see table 1) or by combining the component temperature-dependent functions (for  $\beta$ ,  $A_b^*$  and  $S_b^*$ ; see table 1 and ‘‘Predicting Disease Spread ( $R_0$ ): Methods’’ in the main manuscript).

However, foraging rate ( $f$ ) controls more than just spore removal (the role depicted in eq. [5] and analyzed in the main text). It is also a component of algal ( $A_b^*$ ) and host densities ( $S_b^*$ ) at the boundary equilibrium (eqq. [6a], [6b]). Additionally, it controls parasite contact (since hosts encounter spores while filter feeding; Hall et al. 2007). In the main text, we break down transmission rate ( $\beta$ ) into foraging rate ( $f$ ) and spore infectivity ( $u$ ), according to

$$\beta = f \cdot u \quad (\text{A10})$$

(Strauss et al. 2015). Substituting equations (6a), (6b), and (A10) into equation (5) gives  $R_0$  in terms of the basic component traits so that we can determine how host death rate ( $d$ ), conversion efficiency ( $e$ ), algal growth rate ( $r_A$ ), algal carrying capacity ( $K_A$ ), spore infectivity ( $u$ ), and foraging rate for all traits ( $f_g$ , i.e., global  $f$ ) influence  $R_0$ :

$$R_0 = \frac{d(d - e \cdot f_g \cdot K_A) r_A \cdot u \cdot \sigma_{\max}}{(d + e \cdot f_g \cdot h)(d \cdot r_A - e \cdot f_g \cdot K_A(m + r_A))}. \quad (\text{A11a})$$

We can also apply the substitutions with different symbols for the various roles of foraging rate to determine how foraging rate affects  $R_0$  through its influence on the specific components: spore removal ( $f_z$ , equivalent to  $f$  in eq. [A9c] and the main text, including in fig. 3D), resource-dependent spore production ( $f_\sigma$ ), equilibrium host density ( $f_{Sb^*}$ , which incorporates the effect of resources on host density), and transmission rate ( $f_\beta$ ; fig. A3A):

$$R_0 = \frac{d \cdot f_\beta (d - e \cdot f_{Sb^*} \cdot K_A) r_A \cdot u \cdot \sigma_{\max}}{(d + e \cdot f_\sigma \cdot h)(d \cdot f_z \cdot r_A - e \cdot f_{Sb^*} \cdot K_A(m \cdot f_{Sb^*} + f_z \cdot r_A))}. \quad (\text{A11b})$$

The derivatives for  $R_0$  with respect to each trait scaled per unit of  $R_0$  are

$$\frac{1}{R_0} \frac{\partial R_0}{\partial d} = e \cdot f \left( \frac{h}{d^2 + d \cdot e \cdot f \cdot h} - \frac{K_A \cdot m}{(d - e \cdot f \cdot K_A)(d \cdot r_A - e \cdot f \cdot K_A(m + r_A))} \right), \quad (\text{A12a})$$

$$\frac{1}{R_0} \frac{\partial R_0}{\partial d} = - \frac{e \cdot f^2([d/e \cdot f] + h)(m + (1 - d/[e \cdot f \cdot K_A])r_A)(K_A(-d(d + 2e \cdot f \cdot h) + e^2 \cdot f^2 \cdot h \cdot K_A)m + h(d - e \cdot f \cdot K_A)^2 \cdot r_A)}{(d + e \cdot f \cdot h)^2(1 - d/[e \cdot f \cdot K_A])(d \cdot r_A - e \cdot f \cdot K_A(m + r_A))^2}, \quad (\text{A12b})$$

$$\frac{1}{R_0} \frac{\partial R_0}{\partial r_A} = \frac{e^2 \cdot f^2([d/e \cdot f] + h)K_A(-d + e \cdot f \cdot K_A)m(m + (1 - [d/e \cdot f \cdot K_A])r_A)}{(d + e \cdot f \cdot h)(1 - [d/e \cdot f \cdot K_A])r_A(d \cdot r_A - e \cdot f \cdot K_A(m + r_A))^2}, \quad (\text{A12c})$$

$$\frac{1}{R_0} \frac{\partial R_0}{\partial K_A} = \frac{d \cdot e^2 \cdot f^2([d/e \cdot f] + h)m(m + (1 - [d/e \cdot f \cdot K_A])r_A)}{(d + e \cdot f \cdot h)(1 - [d/e \cdot f \cdot K_A])(d \cdot r_A - e \cdot f \cdot K_A(m + r_A))^2}, \quad (\text{A12d})$$

$$\frac{1}{R_0} \frac{\partial R_0}{\partial u} = \frac{1}{u}, \quad (\text{A12e})$$

$$\frac{1}{R_0} \frac{\partial R_0}{\partial f_g} = - \frac{e^2 \cdot f([d/e \cdot f] + h)(m + (1 - [d/e \cdot f \cdot K_A])r_A)(K_A(-d(d + 2e \cdot f \cdot h) + e^2 \cdot f^2 \cdot h \cdot K_A)m + h(d - e \cdot f \cdot K_A)^2 \cdot r_A)}{(d + e \cdot f \cdot h)^2(1 - [d/e \cdot f \cdot K_A])(d \cdot r_A - e \cdot f \cdot K_A(m + r_A))^2}, \quad (\text{A12f})$$

$$\frac{1}{R_0} \frac{\partial R_0}{\partial f_\sigma} = \frac{e^2 f^2 h([d/e \cdot f] + h)(-d + e \cdot f \cdot K_A)(m + \{f(1 - [d/e \cdot f \cdot K_A])r_A/f\})}{(d + e \cdot f \cdot h)^2(1 - [d/e \cdot f \cdot K_A])(d \cdot f \cdot r_A - e \cdot f \cdot K_A(f \cdot m + f \cdot r_A))}, \quad (\text{A12g})$$

$$\frac{1}{R_0} \frac{\partial R_0}{\partial f_{sb}} = \frac{e^2 f^3([d/e \cdot f] + h)K_A(2d - e \cdot f \cdot K_A)m(m + \{f(1 - [d/e \cdot f \cdot K_A])r_A/f\})}{(d + e \cdot f \cdot h)(1 - [d/e \cdot f \cdot K_A])(d \cdot f \cdot r_A - e \cdot f \cdot K_A(f \cdot m + f \cdot r_A))^2}, \quad (\text{A12h})$$

$$\frac{1}{R_0} \frac{\partial R_0}{\partial f_\beta} = \frac{1}{f_\beta}. \quad (\text{A12i})$$

Host death rate ( $d$ ), conversion efficiency ( $e$ ), maximum algal growth rate ( $r_A$ ), spore infectivity ( $u$ ), and foraging rate as it impacts transmission rate only ( $f_\beta$ ) all increase  $R_0$  with temperature (fig. A3B, A3C). Foraging rate as it impacts spore removal only ( $f_z$ ); foraging rate as it impacts spore production through algal resources ( $f_\sigma$ ); foraging rate as it impacts host density, both directly and indirectly through algal resources ( $f_{sb}$ ); and foraging rate globally ( $f_g$ ) all decrease  $R_0$  with temperature (fig. A3C). Algal carrying capacity has no impact on  $R_0$  (fig. A3B).

## Mesocosm Experiment

### 6. Analysis of Algal Resources

The model (eq. [1]) predicts that equilibril algal density in the absence of disease ( $A_b^*$ ; eq. [6a]) should increase with temperature (fig. 3A). However, in the mesocosm experiment, algal density was lower at 23°C than at 18° or 15°C (fig. 5C). To address this apparent discrepancy, we note that the mesocosm tanks are neither disease free nor at equilibrium. Additionally, the thermal responses of algae that we used to parameterize the model (from Xin et al. 2011) were recorded in different light and nutrient conditions, both of which may interact with temperature.

## Spore Load in Natural Epidemics

### 7. Expanded Methods

We collected samples of hosts, visually diagnosed infection, and calculated weighted lake water temperature as described previously (“Field Survey”). Infected hosts were grouped into small batches (up to 10 animals) and homogenized to

estimate average spore load (counted at  $\times 200$  with a hemocytometer). When there were  $>10$  infected hosts, we averaged multiple batches to produce a single estimate for each combination of lake and date. The data consisted of spore load from 188 lake-date combinations (104 from 2010, 84 from 2014). In the linear mixed effects models, temperature (fixed) was modeled as having (1) a linear relationship with spore yield or (2) a quadratic relationship with spore yield (two linear coefficients, one for temperature and one for temperature squared). Year (fixed) and lake (random) were also included.

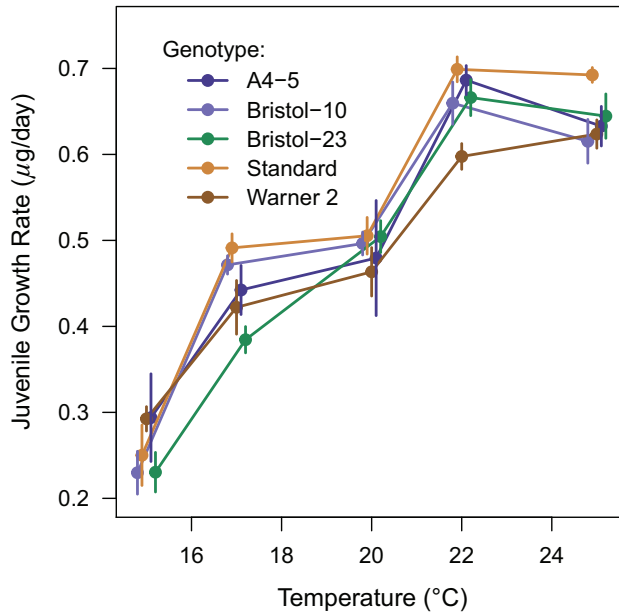


**Figure A1:** Juvenile growth rate for five host clones (including “standard,” the clone used in the trait assays and mesocosm experiment) across temperature. The thermal reaction norms are fairly consistent among clones, although there are some small differences in slopes and optimal temperature. Points are jittered for visual clarity.

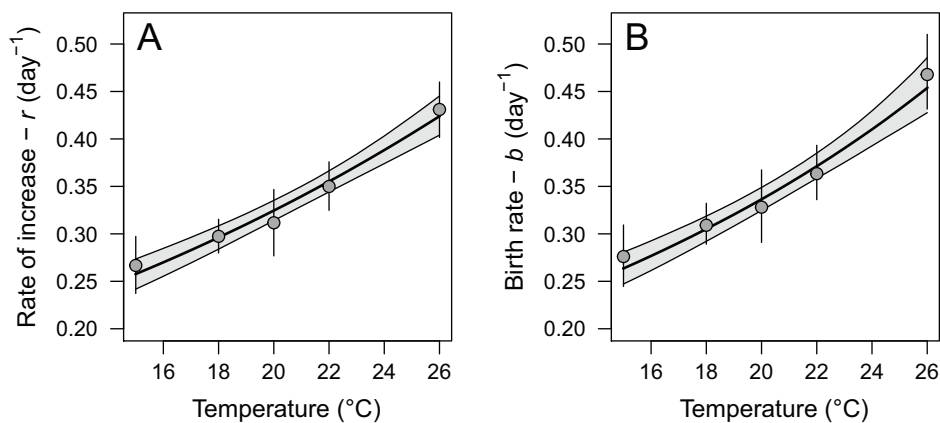


**Figure A2:** Intrinsic rate of increase ( $r$ ; A) and birthrate ( $b$ ; B) of uninfected hosts as functions of temperature (also see table 1). Functions were fit by Bayesian inference. Thick lines are medians of the probability density function; thin lines and gray shading are 95% credible intervals (CI). Points are Bayesian estimates from data at a single temperature treatment (with 95% CI).

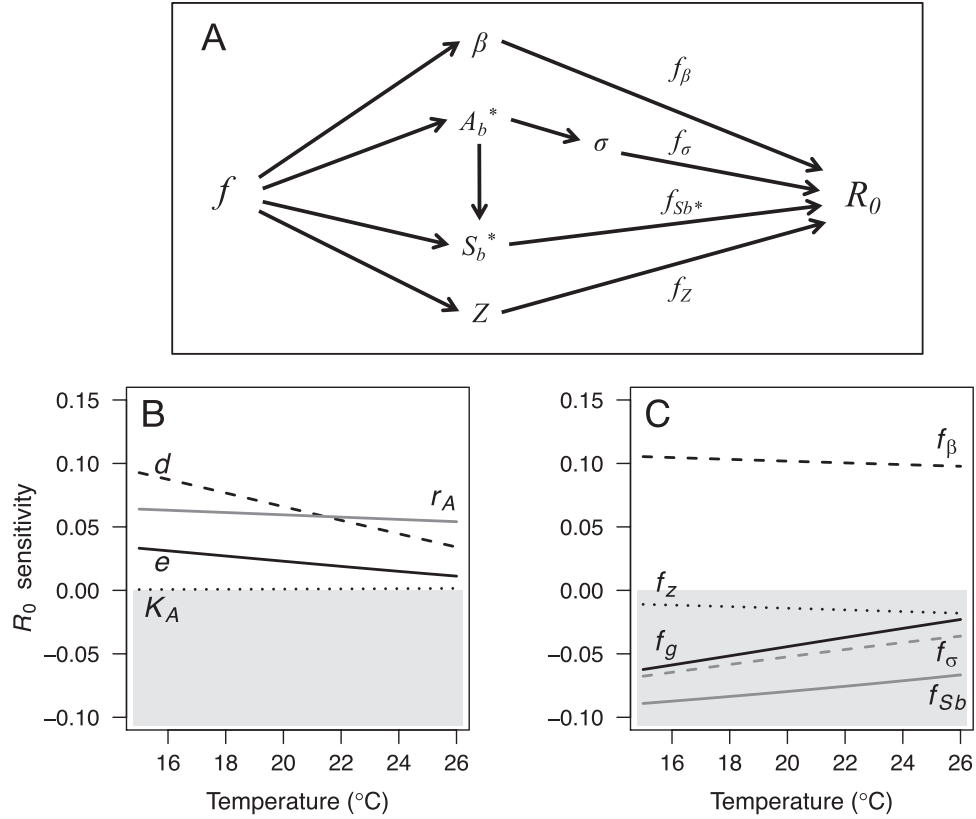


**Figure A3:** *A*, Conceptual diagram of the multiple ways that foraging rate ( $f$ ) affects disease spread ( $R_0$ ). Foraging rate directly influences transmission rate ( $\beta$ ), the boundary equilibrium densities of algae ( $A_b^*$ ) and hosts ( $S_b^*$ ), and spores in the water column ( $Z$ ). It also indirectly influences the density of hosts and spore production ( $\sigma$ ) through algal density. The sensitivity analysis is done at the level of proximate influence on  $R_0$ . Thus, the effect of algal resources on host density are included in  $f_{S_b}$ , while the effect of algal resources on spore production are included in  $f_\sigma$ . *B*, The sensitivity of  $R_0$  to host death rate ( $d$ ), conversion efficiency ( $e$ ), maximum algal growth rate ( $r_A$ ), and algal carrying capacity ( $K_A$ ). *C*, The sensitivity of  $R_0$  to foraging rate globally ( $f_g$ ), foraging rate as it impacts transmission rate only ( $f_\beta$ ), foraging rate as it impacts spore removal only ( $f_Z$ ), foraging rate as it impacts spore production through algal resources only ( $f_\sigma$ ), and foraging rate as it impacts host density, both directly and indirectly through algal resources ( $f_{S_b}$ ). The sensitivity describes the effect of each trait on the value of  $R_0$ . A positive value means the trait is causing  $R_0$  to increase (white area), while a negative value means the trait is causing  $R_0$  to decrease (shaded area).